TNO CONFIDENTIAL

Stieltjesweg 1
2628 CK Delft
Box 155
2600 AD Delft

www.tno.nl

T +31 88 866 20 00
F +31 88 866 06 30

TNO report

| **concept**

Crack noise analysis IJssel bridge A12

Date	September 11, 2018
Author (s)	Sjors van Es Casper Bosschaart Johan Maljaars
Copy number	
Edition	
Number of pages	31 (incl. Attachments)
Number of attachments	
Client	Rijkswaterstaat Attn Sjoerd Wille Box 2232 3500 GE Utrecht
Project name	Fractures toughness
Project number	060.31758 / 01.01

Table of contents

1 preface

Commissioned by Rijkswaterstaat, InfraInspect has been operating since 2017
fatigue inspections performed on details in the IJsselbrug in the A12 nearby
Rheden. The inspector Rijkswaterstaat issued a warning on 3 September 2018
that a crackling sound could be heard in the
near a joint in a side span of the main steel bridge of the
parallel carriageway, in the main girder closest to the right (ie heavy
loaded lane. Following this report, experts from
Rijkswaterstaat visited the bridge on the same day. They have it
said sound also heard and have found that the symmetrical
mirrored connection on the other bank same type of sound but with
increased loudness. Rijkswaterstaat then decided that the
right lane of the parallel lane had to be closed to traffic. The
the main reason for this traffic-limiting measure was the noise
possibly (directly or indirectly) was the result of a growing crack, which
may eventually result in collapse of the bridge construction.

At the time of the report, the bridge was being serviced by the contractor
Hollandia. Rivets were installed near the respective joints
replaced with pretension injection bolts. Because the crackling noise may be one
cause in this work, it was decided to do the work first
(urgently) to be completed, which happened on September 4 and 5. On the night of
A measurement on the bridge took place on 5 September 6, whereby
Rijkswaterstaat has asked TNO for the source of the noise - if it
if it was still present after the work was completed
identify. The sound was observed and the source identified. On
on the basis of this, on 6 September TNO made a constructive adjustment to the
bridge developed, which was installed on 6 and 7 September by contractor Hollandia
in the bridge. In the night of 7 to 8 September, a second measurement is taken on the bridge
took place, whereby it was established that the noise was no longer present and
that the bridge is functioning properly. On the basis of this is in joint
consulted the advice given to remove the traffic restriction, Table 1 .

Table 1 List of activities in chronological order

Date	Activity	stakeholders
9/3/2018	Crackling noise	InfraInspect / RWS
9/3/2018	Set traffic measure	RWS
4 / 5-9-2018	Complete rivet replacement at the concerning locations	Hollandia
5 / 6-9-2018	1 st measurement: identification of sound source	TNO / RWS
9/6/2018	Elaboration of constructive adjustment	TNO
6 / 7-9-2018	Make constructive adjustments	Hollandia
7 / 8-9-2018	2 e measurement: control sound and function the bridge	TNO / RWS
9/8/2018	Advice to cancel a traffic measure	RWS / TNO

This report describes the activities and analyzes performed
by TNO within the framework outlined above. Chapter 2 describes the first
measurement and the result of that measurement. The structural adaptation to the bridge is

described in chapter 3. Chapter 4 describes the second measurement and the result of that measurement. Conclusions and recommendations are given in chapter 5.

2 Noise measurement September 5-6, 2018

2.1 Measurement design

Purpose of the measurement

Acoustic research was carried out on the night of 5-6 September with the aim of achieving this locating the source position of the cracking sound in the monitored sections from the bridge.

The study is limited to two global locations on either side of the river the southern main girder under the parallel runway of the IJsselbrug (direction of travel Arnhem-Westervoort. The motivation for this demarcation arises on the one hand from the perception of the creaking sound at the locations mentioned during work on the bridge and on the other hand due to practical considerations such as the amount of available sensors and time.

Both global locations are equipped with accelerometers. These sensors register vibrations in the steel bridge parts. By the signals from all sensors on simultaneously can be analyzed for a cracking sound which sensor it register the sound first. The position of that sensor is indicative of the source position of the sound.

Locations of the sensors

20 accelerometers have been installed on the Arnhem side of the bridge. The sensor positions are chosen in such a way that it is possible to look in detail at vibrations may have arisen in

- The flange of the main beam
- The lower longitudinal stiffener on the main spar or rivet joints on this location
- The coupling plate over the two webs of the main beam or rivet connections at this location

Furthermore, sensor positions at the edges of the global area have been chosen, among other things rule out a scenario in which the creaking sound is outside the global area arises. Finally, a microphone is placed to hear the audible sound take.

On the Westervoort side of the bridge are 4 accelerometers in a more limited range configuration included to compare the two positions. Also is on placed a microphone on the Westervoort side.

An overview of the sensors on the Arnhem side of the bridge is shown in Figure 2.1 and Table 2.1. There is no overview photo of the Westervoort side available. However, the construction of the bridge is identical. Be on the Westervoort side sensors placed at positions 1,4,14 and 18 as shown in below picture and table. The microphone is on the same on the Westervoort side position.

Figure 2.1 Overview of the sensor positions on the Arnhem side of the bridge.

Table 2.1 Overview numbering accelerometers.

Accelerometer	Position
1.4	Near rivet connection of the profile that the longitudinal stiffeners over the connecting plate, on both sides of the connection between the two webs.
2.5	Close to a rivet connection that connects this profile to the longitudinal stiffener both sides of the connection between the two bodies.
3.6	Bottom horizontal part of the longitudinal stiffener, on both sides of the coupling in the body.
7.8	Marking the top of the global area on the coupling plate between the two webs of the main beam on both sides of the joint.
9.10	Coupling plate between the webs of the main beam on both sides of the link.
11.12	Delineation of the global area on the longitudinal stiffeners.
13.17	On the coupling plate on the top of the flange of the main beam both sides of the connection between the two flanges.
14.18	On the flange of the main beam, just before the coupling plates, on both sides of the connection between the two flanges.
15.19	On the main beam flange, near the cross stiffener weld, on both sides of the connection between the two bodies.
16.20	Delimitation of the global area on the flange, on both sides of the connection between the two bodies.

At all positions are B&K accelerometers with a sensitivity of 1 mV / (m / s $_2$) used.

To attach the accelerometers, the preservative layer of the steel bridge parts removed. The sensor is screwed onto glued sensor feet to be able to bridge the vibrations in the widest possible frequency range measure.

All sensors are connected to B&K LANXy Frontend (A / D conversion) modules. The signals are recorded with a sampling frequency of 131072 Hz sample level to distinguish for the small maturity differences for sensors positioned close together.

After the sensors have been fitted, the entire parallel carriageway is closed at the front traffic and the bridge is subjected to controlled ballast testing. For the

ballast test used two trucks loaded with sand with one total weight of about 50 tons. With these two trucks, the parallel roadway driven in different configurations:
- One truck in the right lane or left lane
- Two trucks in parallel or directly behind each other on the right-hand lane
- Passages at low speed (± 20 km / h) and high speed (± 80 km / h)

2.2 Audible noise

During the passage of the trucks, MEWPs checked whether it was
Crackling noise that was noted on September 3 was still present. This
was carried out by the same experts from Rijkswaterstaat who put the noise on 3
September, with an employee of
TNO. During the measurement, the same crackling noise was heard for both connections
observed as on September 3. In addition, when passing a truck
found in the left lane that the noise was also present - albeit
less hard - in the junction in the beam closest to the left lane
(the lightest loaded beam). Finally, it has been found that the sound too
was present at connections elsewhere in the main beam.

From these noise observations it was concluded that the noise -
directly or indirectly - *could not be* caused by a growing
fatigue crack, which would be a major risk to the safety of the bridge
mean. This conclusion is based on the following facts:
- The type of noise does not match that of a growing fatigue crack; it seemed
  on the so-called 'slip-stick' sound of plates moving over each other. The sound
  therefore cannot be directly caused by a fatigue crack;
- The probability that multiple connections at the same time a fatigue crack
  develop to such an extent that this indirectly ensures what has been established
  sound is very small, therefore practically excluded.
- The main beam near the left lane has historically been much lighter
  varying loads than the main beam near the court
  lane. It is practically impossible that fatigue cracks occur in the same way
  develop time in the left and right main spar.

The locations where the above noise has been detected are all added
passage of a truck both a movement down and to
upstairs. This fits with the suspicion that the sound has to do with 'slip stick'.

2.3 Measurement data and interpretation

During the truck passages for each passage is at both the global location
on the Arnhem side as the Westervoort side of the bridge a cracking sound
observed. For some passages there was also a thumping sound
perceptible. However, the analysis is limited to the creaking sound, because of this
noise is the reason for concern about the bridge and the closure of the parallel track
has been.

To identify the sensor that first records the cracking sound, the
cross correlation between the sensor signals for fragments from the recordings in which
the noise occurs calculated. The cross-correlation is a measure of equality

between two signals, as a function of a mutual shift in time. The
cross correlation has a maximum when the mutual time shift between
two signals correspond to the actual (running) time difference.

This method is very suitable for determining the maturity differences between
sensors that register a sound that originates from one place. To that
condition is always a short fragment with the creaking sound from the
images selected for this analysis.

During the measurement on 5 and 6 September, the
the above-mentioned cross-correlations between the sensors when the

creaking noise calculated. A consistent result is obtained from the maturity differences found forward image in which the creaking sound for each passage arises all around sensors 1-3, and from there extends to the surrounding sensors. For a noise that arises at this position, it is likely that the cause is one or multiple rivets with slight shifting.

Analysis of the sensor group on the Westervoort side of the bridge is also late see that most of the creaking occurs at the sensors on the longitudinal stiffener are confirmed.

This report is not intended to be an exhaustive series of analyzes of each recorded crack, but to further explain the method an example of a typical squat is shown below.

In Figure 2.2 , for a passage of one truck, the graph of the amplitude of acceleration (vibration) as a function of time shown for sensor 3. This sensor is positioned against the horizontal part of the longitudinal stiffener, close to the coupling of the webs of the main beam.

Two sound events are discernible in the recording. The first event in approx the 13 e second, can be described best as a thump, the second event between 14 and 17 seconds sounds like a cracking sound. The fragment between the red lines thus includes the squat, and has been further analyzed by means of a comparison of cross-correlation functions for all accelerometer signals.

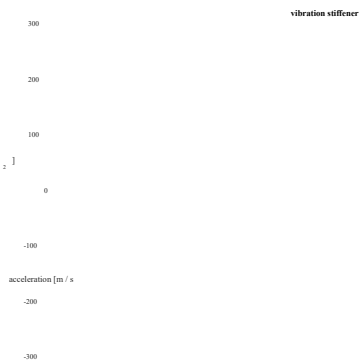

Figure 2.2 Time-amplitude graph of the acceleration, measured on sensor 3 on the body of the longitudinal stiffener. A lump was measured and then creaking.

Figure 2.3 Analysis of the cross-correlation functions for all accelerometers for the cracking fragment between the red lines in Figure 2. 2. The red numbers correspond with the sensor numbers from Table 2.1 .

In the cross-correlation analysis, the sensor signals were compared with the signal of sensor 3. In Figure 2.3 there is one for each sensor on the Arnhem side of the bridge graph of the cross-correlation between that sensor and sensor 3 is shown. The graph of sensor 3 itself, is therefore an autocorrelation.

The graphs of the cross-correlation functions show an image that can be expected for expanding a sound event from one location without notable disturbance from other sounds. Show the cross correlations

clear and unique maxima for a time shift that matches the physical delay due to the transit time of the sound between the sensors.

The transit times are indicated by the difference in samples (discrete steps in the time domain). The number of samples n_s is related to a time difference Δt by the sampling frequency F_s :

Each graph shows the position of the maximum of the cross-correlation function of display that signal with the signal from sensor 3 in terms of the number samples shift from zero found from the autocorrelation from signal 3. A negative number of samples indicates a positive delay for the relevant sensor. That is to say the creaking sound on that sensor *later* is then observed on sensor 3. For a positive difference in samples the creaking sound was detected *earlier* than on sensor 3. As can be seen from above equation, the number of samples is also a measure of the size of the delay. A larger difference therefore indicates a larger time difference.

Figure 2.3 shows that sensors 1,2 and 3 as a cluster are very close to the source of the

sound, and that all other sensors are increasingly distant from the source removed.

3 Constructive adjustment

3.1 Concept solution

The location of the sound at the coupling of the longitudinal stiffener, the geometry of the connection and the nature of the sound that indicated slip-stick makes it it is plausible that the noise was caused by plates in the coupling that are over move each other. From a constructive point of view, the connection was not present optimal because of the uncertainty in the pretensioning force in the rivets and the eccentricity of connection. An alternative connection has been devised, whereby coupling plates are fitted around the current angular stiffener. The coupling plates can be secured to the stiffener. At the location of the coupling plate in the body of the beam a angle profile fitted between the stiffener coupling plates to prevent buckling of the coupling plates. Figure 3.1 shows the geometry of the new through coupling.

Figure 3.1 (Concept) solution stiffener coupling.

On September 6 and 7, contractor Hollandia has the original through-connection removed from the stiffener and the new coupling fitted on site where the sound was best heard.

3.2 Sizing

The following basic principles apply when dimensioning the concept solution used:

- Dimensions of existing construction according to drawings A85.364 and A85.369, folder 4C, bundle 1904.
- Steel type longitudinal stiffeners S235 (derived from Renovation Condition, folder 4B, bundle 1904).
- Sizing based on fully connecting horizontal stiffeners
  - both pull and pressure.
  - Long leg angle force: $_{,} = 150\ 100\ 10 \cdot 150 \quad _{250} \cdot 235 \cdot 10^{-3} = 341$
  - Short leg angle force: $_{,} = 150\ 100\ 10 \cdot 100 \quad _{250} \cdot 235 \cdot 10^{-3} = 227$
- The existing bolt holes in the stiffeners are reused.

- Preload injection bolts, category C. Calculated as preload bolts
  - category C (resistance of injection resin is neglected).
  - Coefficient of friction of the surfaces: $\mu = 0.4$.
- Application of M20 10.9 bolts in large holes ($d_0 = 22$ mm).

Resistance of the individual connectors:

- Shear bolt: $_{,} = \quad _{2} = \dfrac{0.5 \cdot 1000 \cdot 245}{1.25} = 98.0$

- Butt:
  - Long leg angle iron, end bolt: $_{} = \quad _{3_0}; \quad ; 1.0 = \dfrac{45}{3 \cdot 22}; \dfrac{1000}{360}; 1.0 = 0.682$
    $_{1 \cdot \cdots}$
    $_{,} = \quad _{2} = \dfrac{2.5 \cdot 0.68 \cdot 360 \cdot 20 \cdot 10}{1.25} = 98.2$
  - Long leg angle iron, inner bolt: $_{} = \quad _{3_0}; \dfrac{1}{4}; 1.0 = \dfrac{210}{3 \cdot 22} - \dfrac{1}{4}; \dfrac{1000}{360}; 1.0 = 1.00$
    $_{1 \cdot \cdots}$
    $_{,} = \quad _{2} = \dfrac{2.5 \cdot 1.00 \cdot 360 \cdot 20 \cdot 10}{1.25} = 144$
  - Short leg angle iron, end bolt: $_{} = \quad _{3_0}; \quad ; 1.0 = \dfrac{55^{*}}{3 \cdot 22}; \dfrac{1000}{360}; 1.0 = 0.833$
    $_{1 \cdot \cdots}$
    $_{,} = \quad _{2} = \dfrac{2.5 \cdot 0.83 \cdot 360 \cdot 20 \cdot 10}{1.25} = 120$
  - Short leg angle iron, inner bolt: $_{} = \quad _{3_0}; \dfrac{1}{4}; 1.0 = \dfrac{90}{3 \cdot 22} - \dfrac{1}{4}; \dfrac{1000}{360}; 1.0 = 1.00$

* End distance $e_1 = 55$ mm is conservative

$$,= \frac{1 \cdot \cdot \cdot \cdot}{2} = \frac{2.5 \cdot 1.00 \cdot 360 \cdot 20 \cdot 10}{1.25} = 144$$

- Sliding resistance: $, = 0{,}7 \cdot \cdot = 0.7 \cdot 1000 \cdot 245 = 172$ $, = \frac{}{3} \cdot , = \frac{1 \cdot 2 \cdot 0.4}{1.25} \cdot 171.5 = 110$

Resistance of the group of connecting means:
- Long leg angle iron
  - Shear resistance: $4 \cdot , = 4 \cdot 98.0 = 392$
  - Shock resistance: $4 \cdot \cdot = 4 \cdot 0.996 \cdot 97.9 = 391$
  - Sliding resistance $4 \cdot = 1 - \frac{-1^5}{200} = 1 - \frac{315-15 \cdot 20}{200 \cdot 20} = 0.966$ $, = 4 \cdot 110 = 439$
- Short leg angle iron
  - Shear resistance: $4 \cdot , = 4 \cdot 98.0 = 392$
  - Shock resistance: $4 \cdot \cdot „ = 4 \cdot 120 = 480$
  - Sliding resistance $4 \cdot , = 4 \cdot 109.8 = 439$

- Net cross section connecting strips:

  Net cross-section assessment in accordance with NEN-EN 1993-1-1 6.2.3 (4) decisive.
- Strips on long leg angle iron (t = 10 mm):

$$= - 0 \cdot = 95 \cdot 10 - 22 \cdot 10 = 730 \ 2$$

$$, = 2 \cdot \frac{730 \cdot 235 \cdot 10^{-3}}{1.0} = 343$$

- Strips on short leg angle iron (t = 12 mm):

$$= - 0 \cdot = 60 \cdot 12 - 22 \cdot 12 = 456 \ 2$$

$$, = 2 \cdot \frac{456 \cdot 235 \cdot 10^{-3}}{1.0} = 214$$

Buckling of the coupling strips:
- Strips on long leg angle iron (t = 10 mm):

  Buckling length L_{cr} : 0.6 · greatest center-to-center distance between bolts (clamping at bolt)

$$= \frac{}{} = \frac{63.0}{93.0 \cdot 2.89} = 0.232$$

$$= 0.96$$

- Strips on short leg angle iron (t = 12 mm):

  Buckling length L_{cr} : 0.6 · greatest center-to-center distance between bolts (clamping at bolt)

$$= \frac{}{} = \frac{93.0}{93.0 \cdot 3.46} = 0.286$$

$$= 0.98$$

· . Ratio So <0.96

Maximum gross cross-section tension

kink does not occur.

Verification:
- Long leg angle iron with coupling plates 95 · 10 mm 2 (resistance under tension normative):

  Resistance group of connectors: $= \frac{'}{} = \frac{341}{343} = 0.99$ 392 kN

  Resistance net cross-section class C coupling strips: 343 kN
- Short leg angle iron with coupling plates 60 · 12 mm 2 (resistance under tension normative):

  '

Resistance group of connectors: = 227 = 1.06 392 kN
Resistance net cross section class C coupling strips: 214 kN 214

This concerns a small excess in case of tensile load. If NEN-EN 1993-2 NB 8.1.7.1 (2) is applied, the cross-section complies.

Comments:
The implementation of the concept solution on September 6 and 7, 2018 deviates in some degree of sizing described above. As far as is known, this concerns:
- The thickness of all coupling plates is equal to 12 mm. As a result of this the connection of the long legs is more rigid than that of the short legs. The above described thicknesses of 10 and 12 mm are preferred.
- The new angle profile to be fitted has been planed further than indicated in Figure 3.1 to provide sufficient space for existing rivet heads accomplish.

It is further noted that:
- the sketched concept solution has a free length of the longitudinal stiffener required of 595 mm from division into main girders.

This space is not present in all details in the bridge. In some cases the longitudinal stiffener crosses a transverse stiffener at a shorter distance. If the detail an adjustment of the draft solution necessary.
- In many cases the two longitudinal stiffeners to be connected do not fit exactly in each other extended. In the current detailing, this has been compensated by a nod in the corner profile. The proposed draft solution does not include nod. A better result is obtained if this kink is made where necessary applied. The required bend must be measured in the construction.
- The assumed force in the longitudinal stiffener ($f_y \cdot A$) results in a higher one tension in the net cross-section of the longitudinal stiffener. The assumption of full connection therefore conflicts with NEN-EN 1993-1-1 6.2.3 (4).

4 Noise and strain measurement September 7-8, 2018

4.1 Measurement design

4.1.1 Acoustic measurement

The purpose of the acoustic study on the night of September 7-8 is it Determine if a cracking noise is detected after adjusting the connection between the longitudinal stiffeners. If a sound is detected the goal to determine where the sound originates and to make a comparison with the previously perceived sounds.

The design of the noise measurement is almost identical to the measurement at night from 5-6 September, see section 2.1.

After adjusting the connection between the longitudinal stiffeners over the coupling plate connecting the body parts of the main beam is the configuration of the sensors locally adapted. The stiffener is on either side of the joint between the body parts of the main beam equipped with two sensors, namely one sensor on the stiffener body, and a sensor on the flange. This means that sensors 1 and 4 from Figure 2.1 and Table 2.1 are omitted. Positions 2,3,5 and 6 remain enforced. The further sensor configuration on the Arnhem side of the bridge is unchanged.

The sensors on the Westervoort side of the bridge are not for this measurement applied.

Figure 4.1 Adjusted connection of the longitudinal stiffeners and locally adapted configuration of the accelerometers. The sensor numbers correspond to the positions in Table 2.1.

4.1.2 Strain gauge measurement

The noise was detected in the parallel carriageway bridge (PRB), but not - or to a lesser extent - in the bridge of the main carriageway (HRB). This can be an accidental or have a constructive cause. To check whether the constructive behavior of the two bridges are different prior to the ballast strain gauges mounted on a main girder of the PRB bridge and on a main girder of the HRB bridge. When the strain gauges during the ballast tests with the same ballast car there is no difference in constructional effect between the bridges. The strain measurement has a second purpose, which is to validate one structural model of the bridge, drawn up by engineering firm Royal HaskoningDHV (RHDHV). For the purpose of this validation, RHDHV has the Influence line of a point load on the left and right lanes.

The strain gauges are fitted on the underside of the bottom flange of the main girder closest to the right hand lane, just south of the compound where the cracking noise was observed. There are three at this location strain gauges, two in a row in the center of the flange (op a distance from the start of the main bridge of 65.17 m for strips H1 and P4 and 65.37 m for strips H2 and P5) and one at the edge of the flange (outside of the bridge, strips H3 and P6), Figure 4.2. The strain gauges behind each other serve control: these must give an (almost) identical stretch. The strain gauge on the edge of the flange serves to prevent any transverse bending of the flange (due to deformation of the flange from the plane of the main beam). The positions of the strain gauges have been measured and the deviation from the plan (Figure 4.2) was approx. 1 mm, both transversely and lengthways (dat last relative to the biasing bolts in the flange), see Figure 4.3 .

(a) (b)

Figure 4.2 Locations of the strain gauges in relation to the prestressing bolts in the bridge (dimensions in mm): (a) strips H1 to H3 on the HRB bridge; (b) strips P4 to P6 on the PRB bridge.

Figure 4.3 Measuring the locations of the strips.

The lane layout of the PRB bridge has been measured at the junction where the cracking noise has been observed, see Figure 4.4 . This layout will be fine corresponds to the classification used by RHDHV (center of the lanes on 3.625 m / 2 = 1.8125 m from the center of the bridge). The layout of the main carriageway is not measured. The cars have as much as practical in the middle of driven in the lanes, but at the driver's estimate and without re-measurement.

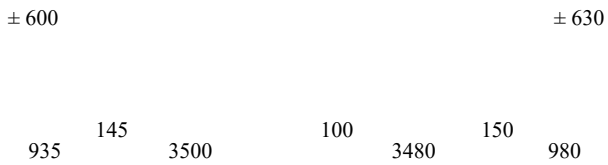

Figure 4.4 Measured lane layout (dimensions in mm).

After the sensors and strain gauges have been installed, the entire parallel road is closed to traffic and the bridge is subjected to controlled ballast testing. Two trucks loaded with sand were used for the ballast test with a total weight of about 50 tons (see tables 4.1 and 4.2). With these two lorries have traveled the parallel road in different configurations:

- One truck in the right lane or left lane
- Two trucks in parallel
- Passages have been carried out at a speed of about 50 km / h

After the passages on the parallel carriageway have been completed, the parallel carriageway has been set up for traffic and the main road is closed. Then on the main carriageway the same passages as on the parallel carriageway, with the exception of the passage where two trucks drive side by side.

One of the two cars was driving on the right lane, the other on the left lane. The masses of the wagons are measured with a weighbridge, Table 4.1 . Table 4.2 shows the distances between the axles of both cars. The distribution of the mass over the axles or wheels is unknown. For the sake of comparison

Between the measurements and the model it is assumed that the front axle is 12% of the total mass and the other axles 22%. Because of the length of the influence line it is the influence of the assumption on the expected elongation is small.

Table 4.1 Masses of ballast wagons.

	Mass car	Mass 2 people (estimate)	Total mass
right strip	48720 kg	140 kg	48860 kg
left strip	49860 kg	140 kg	50000 kg

Table 4.2 Axle distances of ballast wagons.

	front axle - axle 2	axis 2 - axis 3	axis 3 - axis 4	axis 4 - axis 5
right strip	1.94 m	2.09 m	1,345 m	1.25 m
left strip	2.00 m	1.82 m	1.82 m	1.82 m

4.2 Audible noise

At the location where the cracking noise was audible on 3 and 5/6 September and of which the coupling has been replaced, is on the night of 7 to 8 September the same experts from Rijkswaterstaat who heard the sound before from again a cherry picker listened to the bridge. The crackling noise was no longer perceptible. This applied to all truck passages.

4.3 Measurement data and interpretation of noise measurements

By ear the creaking sound seems to have disappeared. By the signal from the to amplify the microphone is just a cracking sound.

The accelerometers also show a cracking sound, it certainly said one factor 40-50 less strong. The amplitude of the loudest creaking noises during a passage occurrence was at 200-250 m / s_2 on the night of September 5-6. After realizing the adaptation, amplitudes of about 5 m / $s_{2\,are}$ found.

An appropriate explanation for perceiving a cracking sound so much less loud is that the noise is eliminated locally, and there is a noise elsewhere the bridge emerges is picked up. This is plausible because at least the A cracking noise has been observed on the west side (see section 2.2). A analysis of the cross correlations of cracking signals for the different sensors shows that there is no consistent image of a hotspot for the creation of it sound occurs more. This result is consistent with a source position outside of it monitored area.

4.4 Measurement data of the strain measurement

The passages of the cars are registered with a sampling frequency of 1000 Hz. The signal contains a harmonic noise with a frequency of 50 Hz and a stretch amplitude of about 5.10^{-6} . This noise is effectively suppressed by after the measurement using a low pass filter of 30 Hz. To illustrate, Figure 4.5 through Figure 4.8 the measurement results of passages of the cars on both lanes of the parallel and main carriageway.

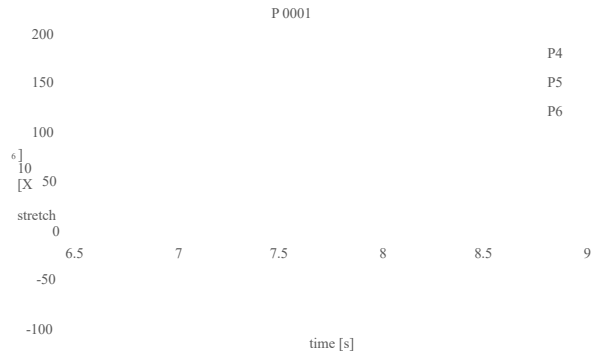

Figure 4.5 Measured racks at passage P 0001 (parallel lane right lane).

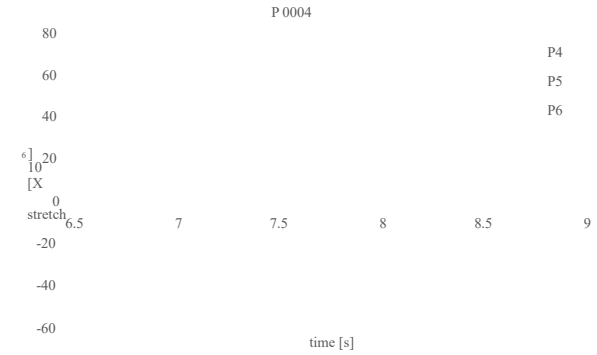

Figure 4.6 Measured elongations at passage P 0004 (parallel lane left lane).

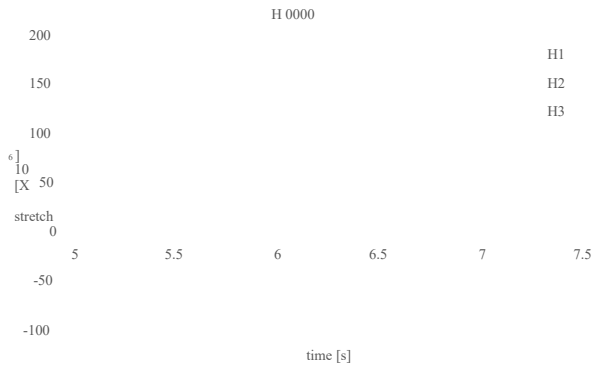

Figure 4.7 Measured racks at passage H 0000 (main lane right lane).

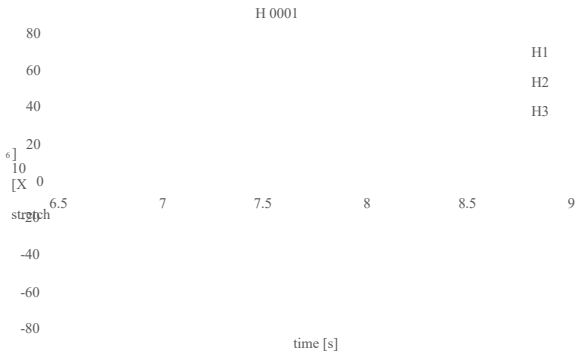

Figure 4.8 Measured racks at passage H 0001 (main lane left lane).

Figures 4.9 to Figure 4.23 give the results per strain gauge of all repeat measurements, in which the strains are converted to stresses assuming a modulus of elasticity of 210,000 MPa. The horizontal axis is expressed in distance, where the speed of the truck is calibrated is that the best match with the model forecast is found. This one calibrated speeds are shown in Table 4.3. In Figure 4.9 to Figure 4.23 also shows the prediction of a model based on the truck configurations and the influence lines for a point load from RHDHV. The influence lines are given for the center of the flange, not for the edge. The measurements of strain gauges H3 and P6 can therefore not be compared with the model. In the figures in question, the model is therefore dotted which in this case is for reference only and not for comparison exact values.

Table 4.3 Calibrated speeds per passage.

Number measurement	Lane wagon	Speed [km / h]
PRB 0001	PRB right lane	55
PRB 0002	PRB left lane	51
PRB 0003	PRB right lane	52
PRB 0004	PRB left lane	50
PRB 0005	PRB right lane	55
PRB 0006	PRB left lane	50
PRB 0007	PRB double	47
HRB 0000	HRB right lane	53
HRB 0001	HRB left lane	50
HRB 0002	HRB right lane	53
HRB 0003	HRB left lane	50

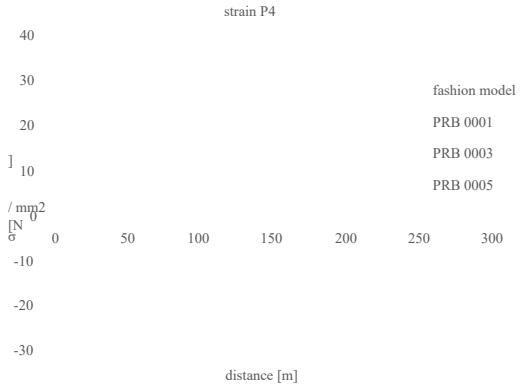

Figure 4.9 Influence lines strain gauge position P4 for passage on the PRB right lane.

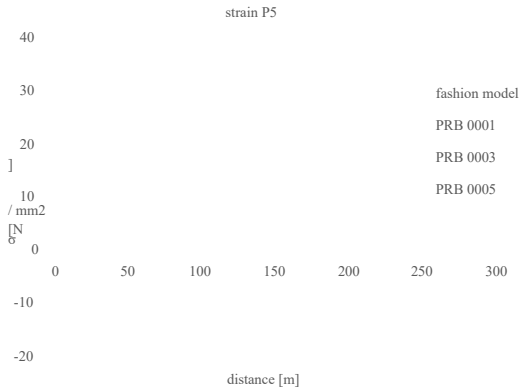

Figure 4.10 Influence lines strain gauge position P5 for passage on the PRB right lane.

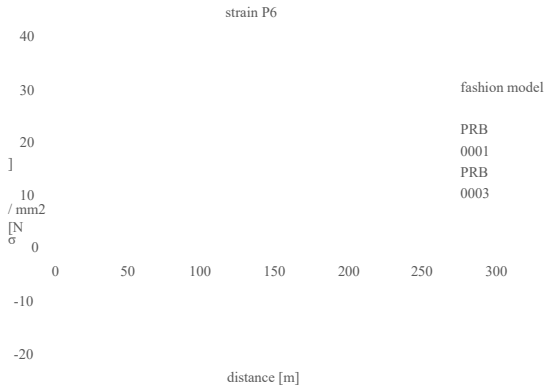

Figure 4.11 Influence lines strain gauge position P6 for passage on the PRB right lane.

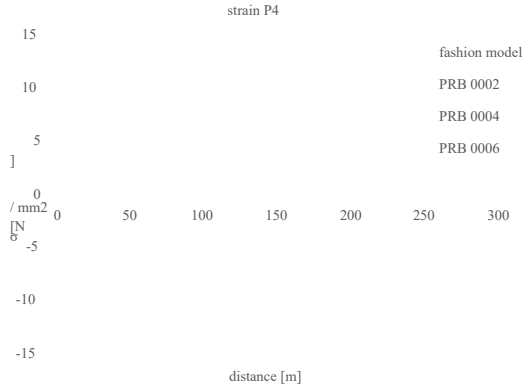

Figure 4.12 Influence lines strain gauge position P4 for passage on the PRB left lane.

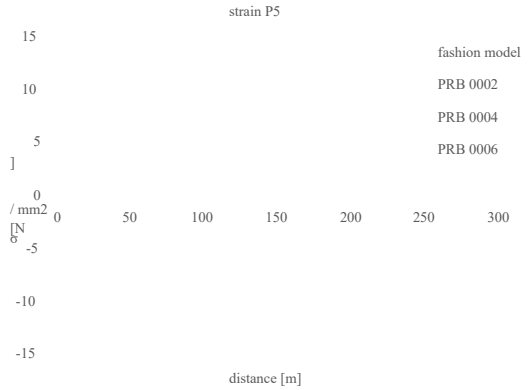

Figure 4.13 Influence lines strain gauge position P5 for passage on the PRB left lane.

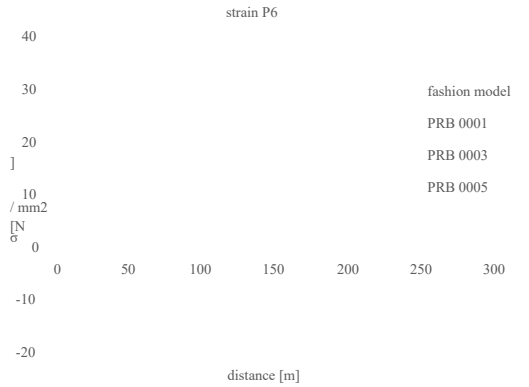

Figure 4.14 Influence lines strain gauge position P6 for passage on the PRB left lane.

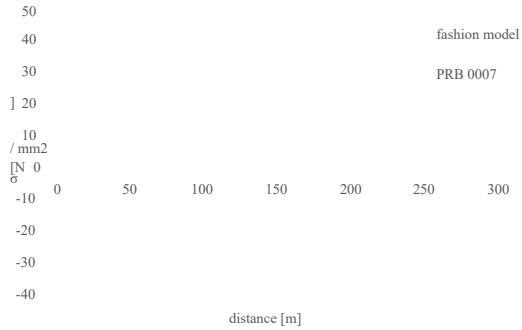

Figure 4.15 Influence lines strain gauge position P4 for passage on the PRB both lanes.

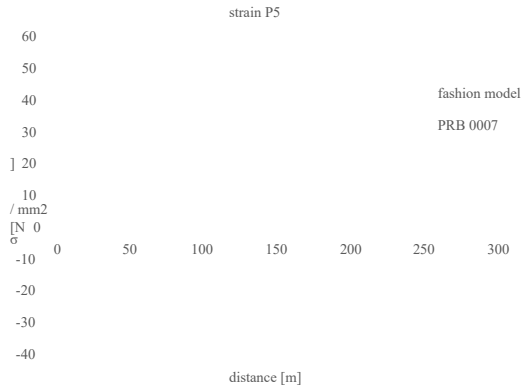

Figure 4.16 Influence lines strain gauge position P5 for passage on the PRB both lanes.

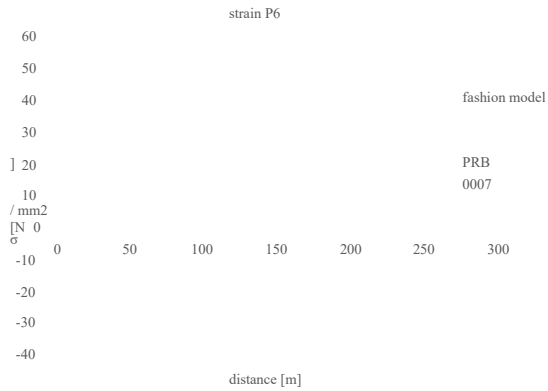

Figure 4.17 Influence lines strain gauge position P6 for passage on the PRB both lanes.

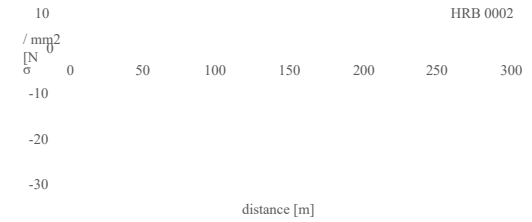

Figure 4.18 Influence lines strain gauge position H1 for passage on the HRB right lane.

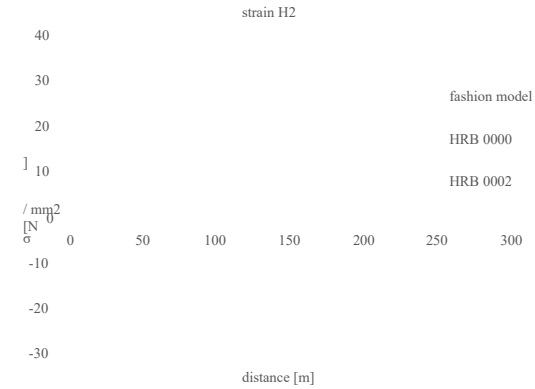

Figure 4.19 Influence lines strain gauge position H2 for passage on the HRB right lane.

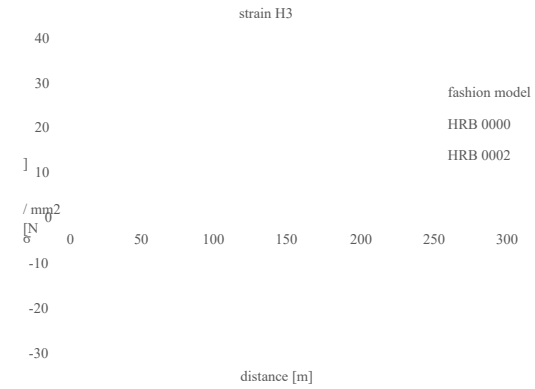

Figure 4.20 Influence lines strain gauge position H3 for passage on the HRB right lane.

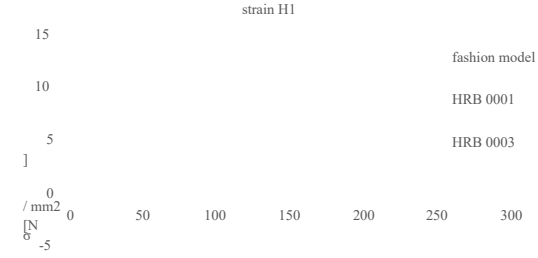

Figure 4.21 Influence lines strain gauge position H1 for passage on the HRB left lane.

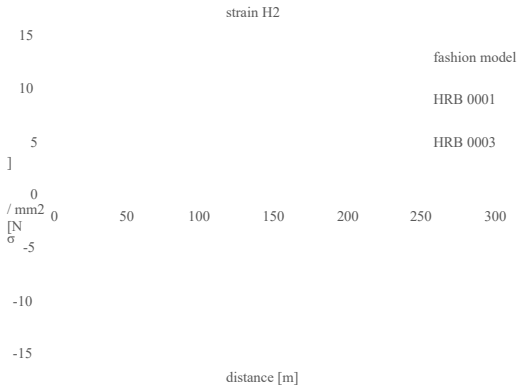

Figure 4.22 Influence lines strain gauge position H2 for passage on the HRB left lane.

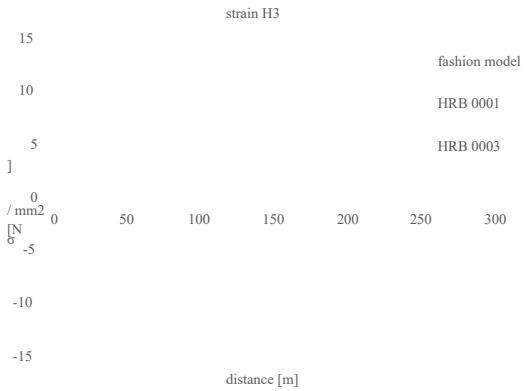

Figure 4.23 Influence lines strain gauge position H3 for passage on the HRB left lane.

Table 4.4 gives the result of the measurements in terms of the maximum voltage range, the maximum value and the minimum value of the measurements per strip (columns 2 to 6) and the model (column 7). Column 8 gives the ratio between model and measurement. Column 9 gives the relationship between the strain gauges P5 and P6 and between H2 and H3, which gives an idea of the influence of 'cross bending' (bending out of plane) of the beam flange. Column 10 gives the ratio between the strain gauges P4 and P5 and between H1 and H2, which gives an idea of the influence of the variation in measured strains over the 200 mm distance between the strain gauges longitudinal direction of the bridge.

Table 4.4 Maximum ranges, maxima and minima of the stresses in MPa according to measurements and models at the truck passages.

Range	individual measurements			avg. measurement μ	var. measurement V	model	model / μ measurement	transverse bending	length-variation
PRB right	PRB 0001	PRB 0003	PRB 0005						
P4	54.8	54.6	55.7	55.1	0.010	53.0	0.96		
P5	52.5	52.4	53.4	52.8	0.011	53.0	1.00		1.04
P6	52.3	52.0	53.0	52.4	0.009			0.99	
HRB right	HRB 0000	HRB 0002							
H1	53.3	52.7		53.0	0.007	53.0	1.00		
H2	52.7	52.2		52.5	0.007	53.0	1.01		1.01
H3	52.5	52.1		52.3	0.005			1.00	
PRB left	PRB 0002	PRB 0003	PRB 0006						
P4	21.6	21.2	22.2	21.7	0.022	26.4	1.22		
P5	20.7	20.4	21.3	20.8	0.023	26.2	1.26		1.04
P6	25.0	24.7	25.5	25.1	0.015			1.21	
HRB left	HRB 0001	HRB 0003							
H1	22.4	23.2		22.8	0.026	26.4	1.16		
H2	22.4	23.3		22.8	0.028	26.2	1.15		1.00
H3	26.2	27.0		26.6	0.020			1.16	

Maximum individual measurements				avg. measurement μ	var. measurement V	model	model / μ measurement	transverse bending	length-variation
PRB right	PRB 0001	PRB 0003	PRB 0005						
P4	37.4	37.7	38.3	37.8	0.013	36.1	0.96		

P5	35.8	36.0	36.6	36.1	0.012	35.9	0.99		1.05
P6	35.3	35.6	36.1	35.7	0.011			0.99	
HRB right HRB 0000 HRB 0002									
H1	35.9	35.5		35.7	0.008	36.1	1.01		
H2	35.3	34.9		35.1	0.008	35.9	1.02		1.02
H3	35.0	34.8		34.9	0.006			0.99	
PRB Links PRB 0002		PRB 0003	PRB 0006						
P4	11.6	11.3	12.3	11.7	0.041	14.3	1.22		
P5	11.1	10.8	11.8	11.2	0.042	14.3	1.27		1.04
P6	14.3	14.1	14.8	14.4	0.024			1.28	
HRB left	HRB 0001 HRB 0003								
H1	11.8	12.5		12.1	0.039	14.3	1.18		
H2	11.8	12.5		12.2	0.045	14.3	1.18		1.00
H3	14.7	15.3		15.0	0.027			1.23	

Minimum individual measurements				**avg. measurement μ**	**var. measurement V**	**model**	**model / μ measurement**	**transverse bending**	**length-variation**
PRB right PRB 0001		PRB 0003	PRB 0005						
P4	-17.4	-16.9	-17.4	-17.3	-0.016	-16.9	0.98		
P5	-16.7	-16.4	-16.8	-16.6	-0.013	-17.1	1.03		1.04
P6	-16.9	-16.4	-16.9	-16.7	-0.015			1.01	
HRB right									
H1	-17.4	-17.2		-17.3	-0.005	-16.9	0.98		
H2	-17.4	-17.3		-17.4	-0.004	-17.1	0.98		0.99
H3	-17.4	-17.3		-17.4	-0.004			1.00	
PRB Links									
P4	-10.0	-9.9	-9.9	-9.9	-0.002	-12.1	1.22		
P5	-9.6	-9.5	-9.6	-9.6	-0.002	-12.0	1.25		1.04
P6	-10.7	-10.6	-10.7	-10.7	-0.004			1.12	
HRB left									
H1	-10.6	-10.8		-10.7	-0.011	-12.1	1.13		
H2	-10.6	-10.7		-10.7	-0.010	-12.0	1.12		1.00
H3	-11.5	-11.7		-11.6	-0.012			1.09	

4.5 Interpretation of the strain measurement

The repeat measurements showed almost identical stretches at similar ones ballast tests, so the measurements are easily reproducible. This follows from the measurement the maximum ranges, maxima and minima of the measured racks are good for the main carriageway and the parallel carriageway (difference of the order of 2%). So there is no difference in constructional effect between the bridges.

The measured stretches show a ripple with a frequency of approximately 2 Hz and an amplitude of up to approx. 1 MPa over the entire course of the passage. This ripple is the same with every passage. This ripple is attributed vibrating the bridge in a eigenmode, which is nudged by the passage of the car.

The measurements with a ballast test on the right-hand lane correspond well to the model (deviation 2 to 4%). For the left lane there is a significant difference found between the measurements and the model, where the model has a 22 to 27% predicts higher voltage than what is measured.

If it is assumed that the payment to the main beams is proportional with the distance to the center of the lane (so without cooperation between the beams, according to a two-dimensional model) follows a ratio in the tension in the main beam to which the strain gauges are applied between loads on the left strip and on the right strip of 0.25. According to the measurement, this is ratio about 0.39 and according to the model 0.50. This means that the beams do collaborate. Due to the presence of the relationship between the beams both main beams pulled. Based on the measurement, the however cooperation in the model is overestimated. A first explanation for this is that the connections to the bridge may be too rigid. This stiffness can affect the distribution between the main girders, the sum of it

this is not expected to have a tax effect on both main beams
significantly affected. If this statement is correct, this would be the case when modeling
less rigid connections, so the load effect on both beams is slightly overestimated
turn into. This can be explained by the disk action of the relatively high beams and the
curved bottom flange. Both aspects are not included in the model.

It follows from comparison of strain gauges P5 with P6 and of H2 with H3
transverse bending effect when passing the lorry over the right lane: the
tension at the edge of the flange is identical to that in the heart. When passing over
in the left lane a significant transverse bending effect has been measured. The
voltage change measured in the strain gauge near the edge of the flange is approx. 4 MPa
or 20% higher than those in the heart. With the double passage - with a car on
the left and right lanes - is the same increase in the
voltage change near the edge to the heart of 4 MPa (in that
this is 5% of the total voltage change). Because the strain gauge is not
it is exactly on the edge, but 15 mm away from it, it is
transverse bending effect at the edge of the flange a factor (250 / (250-15) =) 1.06 higher
then measured.

The racks of strips P4 and P5 - both at the heart of the flange of the
parallel carriageway at a distance of 200 mm - differs approx. 4%. A
such a stretch difference is not expected, is not found in the model of
RHDHV and is also not found between lanes H1 and H2 of the main carriageway.
This suggests that it is a measurement inaccuracy. The
measuring instruments and the data acquisition system have a much larger one
accuracy and cannot be the source of this difference. A possible
explanation is that strip 5 (and strip 6) is not / are not exactly lengthwise
applied. The angle φ by which the strain gauge must be rotated relative to
the longitudinal direction to explain the difference in elongation follows from:

$$\text{rack P5}_{\text{rackP4}} = \cos - \nu \sin \quad (4.1)$$

For a cross contraction coefficient ν = 0.3 and a stretch ratio of 0.96 follows
an angle φ = 6 degrees. It is conceivable that strip 5 (and strip 6) should be under one
such an angle with respect to the longitudinal direction.

5 Conclusions

On 3 September, Rijkswaterstaat was warned by an inspector that the IJssel bridge in the A12 produces a cracking noise at the site of a connection in the bridge of the parallel road, at the passage of trucks. Further research by Rijkswaterstaat found that the noise was at least one other connection also occurred. As a precaution, Rijkswaterstaat has a lane off the bridge closed to traffic.

Rivets near those joints were replaced with preload injection bolts at the time of the cracking noise observation. Because the Crackling noise may have had a cause in this work, it was decided to remove the complete work (urgently) first, which happened on 4 and 5 September.

To check whether the sound was still present and if so, what the source TNO had accelerometers and microphones on 5 September mounted on the bridge near the joints where the noise was perceived. A measurement was taken in the night of 5 to 6 September whereby ballast wagons have driven over an otherwise empty bridge. The noise became observed and the source was identified with the accelerometers.

The noise came from the connection in the lower longitudinal stiffener where the body is connected. Based on this, TNO has 6 In September, a constructive adaptation to this longitudinal stiffener was developed, which was installed by contractor Hollandia on 6 and 7 September.

On September 7, TNO again installed accelerometers and microphones and

also strain gauges mounted on a main girder of the bridge of the
parallel carriageway and at the same location of the bridge from the main carriageway. During the night
from 7 to 8 September has a second measurement with ballast wagons on both
bridges took place, which was determined on the basis of the accelerometers
that the sound was no longer present. In addition, based on the
strain gauge measurements concluded that there was no difference in stretching between the
bridge of the parallel carriageway and that of the main carriageway. Based on that, in
joint consultation between RWS and TNO advised giving the
to remove traffic restrictions.

The strain gauge measurements served, in addition to checking whether the bridges were the same
exhibit constructive behavior, including a calculation model from engineering firm Royal
HaskoningDHV to check. When passing a car on the lane that is
is closest to the measured main beam is a good match
found between the calculation model and the measurement (difference about 1%). For the others
lane gives the model an approximately 25% higher voltage than the measurement.

6 Signature

Delft, October 2018	TNO
Dr. PC Rasker	Dr.ir. SHJ van Es Ir. C. Scissors Prof.dr.ir. J. Maljaars
Department head	Author